# PVAm–PIP/PS Composite Membrane with High Performance for $CO_2/N_2$ Separation

**Zhihua Qiao, Zhi Wang, Chenxin Zhang, Shuangjie Yuan, Yaqun Zhu, and Jixiao Wang**
Chemical Engineering Research Center, School of Chemical Engineering and Technology, Tianjin University, Tianjin 300072, P.R. China

State Key Laboratory of Chemical Engineering, Tianjin University, Tianjin 300072, P.R. China

Dept. of Chemical Engineering, Tianjin Key Laboratory of Membrane Science and Desalination Technology, Tianjin University, Tianjin 300072, P.R. China

**Shichang Wang**
Chemical Engineering Research Center, School of Chemical Engineering and Technology, Tianjin University, Tianjin 300072,P.R. China

Dept. of Chemical Engineering, Tianjin Key Laboratory of Membrane Science and Desalination Technology, Tianjin University, Tianjin 300072, P.R. China

*DOI 10.1002/aic.13781*
*Published online March 19, 2012 in Wiley Online Library (wileyonlinelibrary.com).*

*Polyvinylamine (PVAm) was modified using a cross-linking agent containing carriers piperazine (PIP). Attenuated total reflectance fourier transform infrared, elemental analyzer, and X-ray diffraction were used to characterize the PIP-modified PVAm. The PVAm–PIP/polysulfone (PS) composite membrane was developed by coating PVAm–PIP mixed solutions with different mass ratios of PIP/PVAm ($m_{PIP}/m_{PVAm}$) on the PS ultrafiltration membrane. The effects of $m_{PIP}/m_{PVAm}$ (from 0.715 to 2.860) in the coating solutions and wet coating thickness on the gas performance of the PVAm–PIP/PS composite membrane were investigated. The PVAm–PIP/PS composite membrane prepared showed higher performance than other membranes reported in the literature due to the large increase of the introducing carrier concentration and low crystallinity. Moreover, the separation performance stability of the PVAm–PIP/PS composite membrane was investigated and no deterioration in the membrane permselectivity was observed. Finally, the economic evaluation of the membrane with the highest performance prepared was carried out.*  *AIChE J,* 59: 215–228, 2013
*Keywords: fixed carrier membrane, piperazine, cross-linking, polyvinylamine, $CO_2$ permeance, $CO_2/N_2$ selectivity*

## Introduction

Modern membrane technology for $CO_2$ capture has been attracting more and more attention nowadays because the membrane-based $CO_2$ separation process has well-known advantages of low-energy consumption, operational simplicity, and low pollution over other techniques.[1–6] The membrane is the key of the membrane separation process. The permeance and selectivity are two important parameters of the membrane. To define the feasible performance of the polymer membrane that could meet the techno-economical requirement for $CO_2$ capture, considerable research efforts have been made in recent years.[7–11] To fulfill the separation target of $CO_2$ purity $>$ 95% and $CO_2$ recovery $>$ 90% from postcombustion gas (15% $CO_2$ in the mixed gas),[12] the simulation results in our previous work show that the minimum selectivity required for the single-stage membrane system is 300 under an extreme condition that the pressure ratio (the permeate pressure to the feed pressure) approaches 0.[11] For the two-stage membrane system with a recycle stream, the minimum selectivity would decrease to 40 with the pressure ratio of 0.05 to fulfill the membrane separation target. The two-stage membrane system with a recycle can be a cost-competitive alternative method if the membranes have $CO_2/N_2$ selectivity of 52 and $CO_2$ permeance of 0.13735 $\mu$mol/($m^2$ s Pa) or $CO_2/N_2$ selectivity of 75 and $CO_2$ permeance of 0.061305 $\mu$mol/($m^2$ s Pa).[11] However, commercially available polymer membranes such as cellulose acetate, polysulfone (PS), silicon rubbers, polyamides, and polyimides, which hardly have high $CO_2$ permeance and $CO_2/N_2$ selectivity simultaneously, could not meet the requirement for $CO_2$ capture. Recently, some ultrathin membranes showed an encouraging $CO_2$ permeance more than 0.067 $\mu$mol/($m^2$ s Pa).[13–17] The membrane proposed by Merkel showed $CO_2$

Correspondence concerning this article should be addressed to Z. Wang at wangzhi@tju.edu.cn.

permeance as high as 0.335 $\mu$mol/(m$^2$ s Pa).[18] However, the $CO_2/N_2$ selectivity of these membranes is generally no more than 55. Consequently, to meet the requirement for $CO_2$ capture, the membrane with high $CO_2$ permeance and high $CO_2/N_2$ selectivity has become a strong subject of research interest.[19]

Fortunately, a high $CO_2$ permeance and a high $CO_2/N_2$ selectivity can be obtained simultaneously in the fixed carrier membrane through the reversible reaction between the reactive carrier and the targeted gas–$CO_2$. In the $CO_2/N_2$ separation process, $CO_2$ transports through the fixed carrier membrane following ordinary diffusion which corresponds to the contribution from solution-diffusion of uncomplexed $CO_2$ and facilitated transport which corresponds to the contribution from reaction–diffusion of $CO_2$–carrier complex, whereas $N_2$ transports through the fixed carrier membrane only following ordinary diffusion which corresponds to the contribution from solution-diffusion of $N_2$.[20] Inspired by the amine absorption process, carriers of the fixed carrier membrane for $CO_2$ separation are mainly amine groups contained in polymers. The gas performance of the fixed carrier membrane is influenced by crystallinity because $CO_2$ and $N_2$ cannot transport through the crystalline region and the amine carriers in the crystalline region cannot react with $CO_2$.[21–23] Therefore, only the amine carriers in the amorphous region, which are called effective carriers, can react with $CO_2$, and improving the concentration of the effective carriers has an important effect on the performance of the fixed carrier membrane.[24] Some polymers containing amine groups such as polyvinylamine (PVAm),[24–32] polyallylamine,[33,34] and polyethylenimine[35] have been used to prepare the fixed carrier membrane. PVAm (Figure 1) as a simple fixed carrier membrane material has been studied for $CO_2$ separation for many years and the membrane containing PVAm presented higher performance compared with the available polymer membrane.[24–32] However, the concentration of effective carriers in the PVAm membrane is not easy to be improved. This is caused by two reasons. One is that the carrier concentration in the PVAm is not high, and the other is that the crystallinity of the pure PVAm is high.[24] Hence, the performance of the membrane containing PVAm reported in the literature could not well meet the requirement for $CO_2$ capture.[11]

In our previous work, a new idea of modifying the fixed carrier membrane for $CO_2/N_2$ separation by a cross-linking agent containing carriers to simultaneously improve $CO_2$ permeance and $CO_2/N_2$ selectivity was suggested and proved to be feasible.[20] Following the above idea, the PVAm–ethylenediamine (EDA)/PS composite membrane was prepared. The PVAm–EDA/PS composite membrane with an ultrathin selective layer presented the maximum of $CO_2$ permeance of 0.203345 $\mu$mol/(m$^2$ s Pa) and $CO_2/N_2$ selectivity of 106. However, there are two problems when PVAm was modified

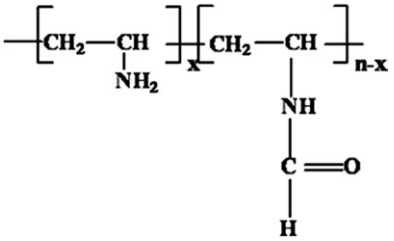


**Figure 1. Chemical structure of PVAm.**

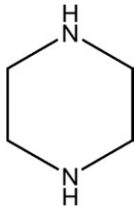


**Figure 2. Chemical structure of PIP.**

by EDA. (1) The EDA is easily volatile, thus, the concentration of introducing carriers by EDA cross-linking PVAm in the PVAm–EDA/PS composite membrane is difficult to be largely improved. (2) With the increase of the mass ratio of EDA/PVAm ($m_{EDA}/m_{PVAm}$) in the coating solution from 0 to 5, the crystallinity of the PVAm–EDA/PS composite membrane increases rapidly. Consequently, the effective carrier concentration in the PVAm–EDA/PS composite membrane is difficult to be largely improved.[20]

In this work, to gain the fixed carrier membrane with high performance and well meet the requirement for $CO_2$ capture, piperazine (PIP) (Figure 2) was chosen as a new cross-linking agent to modify PVAm. On one hand, PIP is not easily volatile, thus, the concentration of introduced carriers by PIP cross-linking PVAm in the PVAm–PIP/PS composite membrane may be higher than that in the PVAm–EDA/PS composite membrane. On the other hand, different from EDA with the regular and symmetric structure, two secondary amine groups of PIP are fixed by the chains with a heterocyclic and noncoplanar structure. Hence, the crystallinity of the PVAm–PIP/PS composite membrane may be lower than that of the PVAm–EDA/PS composite membrane, and the effective carrier concentration in the PVAm–PIP/PS composite membrane may be higher than that in the PVAm–EDA/PS composite membrane. Therefore, the PVAm–PIP/PS composite membrane may have higher $CO_2$ permeance and $CO_2/N_2$ selectivity than the PVAm–EDA/PS composite membrane.

The PVAm–PIP/PS composite membrane with an ultrathin selective layer prepared in this work presented the maximum of $CO_2$ permeance of 2.1775 $\mu$mol/(m$^2$ s Pa) and $CO_2/N_2$ selectivity of 277, which is much higher than the maximum performance of the PVAm–EDA/PS composite membrane. The economic evaluation of the membrane with the highest performance prepared in this work was carried out. The results show that the two-stage membrane system using the membrane prepared in this work has the economic feasibility of $CO_2$ capture from large emission sources.

## Experimental

### *Materials*

N-vinylformamide from Aldrich was distilled under vacuum and stored at $-15^\circ$C. 2,2′-Azobis (2-methylpropionamidine) dihydrochloride from Aldrich was recrystallized from ethanol and stored at $-15^\circ$C. The PS ultrafiltration membrane with an average cutoff molecular weight of 6000 was supplied by Vontron Technology, China. 201×7 strongly basic anion exchange resin was purchased from Chemical Plant of Nankai University (China) and regenerated before using. PIP (99.0% purity) was obtained from Aladdin Reagent (China) and used without further purification. Ethanol and hydrochloric acid (HCl) were of analytical grade and used as received.

### *Preparation of composite membranes and films*

PVAm was obtained according to a method in the reference.[20] PVAm–PIP coating solutions containing 20 kg/m$^3$ PVAm as well as 14.5, 29, and 58 kg/m$^3$ PIP were prepared by mixing 3 wt % PVAm aqueous solutions with various amounts of PIP and deionized water. Then, the mixtures were stirred for 12 h and stood for 24 h. The PVAm–PIP/PS composite membrane was prepared by coating the PVAm–PIP mixed solution with different mass ratio of PIP/PVAm ($m_{PIP}/m_{PVAm}$) on the PS ultrafiltration membrane with a preset wet coating thickness (the gap between substrate and coating knife) by a coating applicator with an accuracy of $\pm 10$ $\mu$m, followed by drying at 30°C and 40% relative humidity in an artificial climate chamber (Climacell 222R, Germany) at least 24 h. In this work, PVAm–PIP blend is a separation layer, and the PS ultrafiltration membrane acts as a support layer. To eliminate the effect of the PS ultrafiltration membrane and well characterize PVAm–PIP blend, the PVAm–PIP film for characterization was prepared. The PVAm–PIP film was obtained by coating the PVAm–PIP mixed solution on the silicone rubber substrate, then drying for 24 h under the same temperature and humidity as mentioned above, and finally peeling from the silicone rubber substrate.

### *Characterization and measurement*

*Characterization of Films.* The chemical characterization of the PVAm–PIP film was accomplished by attenuated total reflectance fourier transform infrared (ATR-FTIR) spectrometer (FTS-6000, Bio-Rad of America). The mass ratio of C/N ($m_C/m_N$) in the film with different $m_{PIP}/m_{PVAm}$ in the coating solution was measured by an elemental analyzer (Carlo Erba EA1110, Italy). The $m_{PIP}/m_{PVAm}$ in the PVAm–PIP films was calculated according to $m_C/m_N$ in the films. The drying retention degree (DRD) of PIP in the PVAm–PIP film was calculated according to the $m_{PIP}/m_{PVAm}$ in the coating solution and PVAm–PIP film. The DRD of PIP in the film is defined as the mass ratio of PIP/PVAm in the drying PVAm–PIP film to that of PIP/PVAm in the coating solution. The formula is given as follows

$$DRD(\%) = \frac{(m_{PIP}/m_{PVAm})_{film}}{(m_{PIP}/m_{PVAm})_{solution}} \times 100\% \quad (1)$$

where $(m_{PIP}/m_{PVAm})_{film}$ and $(m_{PIP}/m_{PVAm})_{solution}$ are the mass ratio of PIP/PVAm in the drying PVAm–PIP film and in the coating solution, respectively.

The thermal stability of PIP in the PVAm–PIP film was represented by the heat-treated retention degree (HRD). The $m_C/m_N$ in the PVAm–PIP film heat-treated under vacuum and untreated PVAm–PIP film was measured by the elemental analyzer mentioned above. The HRD was calculated according to the $m_{PIP}/m_{PVAm}$ in the PVAm–PIP film heat-treated under vacuum and untreated PVAm–PIP film. The PVAm–PIP film was heat treated at 30, 80, 100, and 150°C, respectively, under vacuum until the film reached a constant weight. The HRD is defined as the mass ratio of PIP/PVAm in the PVAm–PIP film heat-treated under vacuum to that in the untreated PVAm–PIP film, respectively. The formula is given as follows

$$HRD(\%) = \frac{(m_{PIP}/m_{PVAm})_{\times °Cvacuum}}{(m_{PIP}/m_{PVAm})_{film}} \times 100\% \quad (2)$$

where $(m_{PIP}/m_{PVAm})_{\times °Cvacuum}$ and $(m_{PIP}/m_{PVAm})_{film}$ are the mass ratio of PIP/PVAm in the PVAm–PIP film heat-treated at X°C under vacuum and untreated PVAm–PIP film, respectively.

The crystallinity of the PVAm–PIP film was investigated by X-ray diffraction (XRD) spectra using an X-ray diffractometer (D/MAX-2500) in the reflection mode with $2\theta$ scanned between 5° (0.087 rad) and 80° (1.40 rad) under an 8 kW power.

*Characterization and Measurement of Membranes.* Scanning electron microscope (SEM) images of the surface and the cross-section for the PVAm–PIP/PS composite membrane were obtained on Nova NanoSEM 430 (FEI). For the cross-section observation, the membrane sample was prepared by peeling away the polyester fabric, then frozen in liquid nitrogen and fractured. All membrane samples were coated with gold by a sputter-coating machine.

The permeance and the selectivity of the PVAm–PIP/PS composite membrane were measured by a set of test equipment[36] using $CO_2/N_2$ mixed gas (20/80 by volume). The membrane was mounted in a circular stainless steel cell (effective membrane area = 19.26 cm$^2$). Before contacting the membranes, the feed gas was saturated with water vapor by bubbling through water bottles at 30°C and then passing an empty bottle at room-temperature (22°C) to remove the condensate water. The sweep gas ($H_2$) in the permeate side was humidified by passing through water bubblers at room-temperature (22°C). The outlet sweep gas composition was analyzed by a gas chromatograph equipped with a thermal conductivity detector. The sweep process is usually used in the laboratory for the convenience of the test.[18,20,24,31–33] The use of a humidified downstream sweep, vs. an actual permeate side that would be used in real situations, causes the downstream membrane face to remain hydrated and causes the membrane to show a much more attractive high $CO_2$ permeance and $CO_2/N_2$ selectivity. The permeance of $CO_2$ and $N_2$ was calculated from the sweep gas flow rate and its composition. The downstream pressure in the apparatus was maintained at the atmosphere pressure. The gas permeance is customarily expressed in the unit of $\mu$mol/(m$^2$ s Pa). Most of the $CO_2/N_2$ separation membrane was tested at room-temperature in literatures.[13,14,18,20,31] For the comparison with other membranes in literatures, the PVAm–PIP/PS composite membrane was tested at room-temperature (22°C) with a feed pressure varying from 0.11 to 1.6 MPa, and steady-state permeation was assumed to have been reached when the sweep gas flow rate and its composition no longer changed with time. However, for the $CO_2/N_2$ separation membrane, $CO_2$ capture from flue gas is an important application. The temperature of the true operating flue gas is about 40–50°C in a real plant.[36] Hence, the effect of the temperature on the performance of the membrane was investigated, and the performance stability of the membrane was investigated at 50°C as well as at room-temperature (22°C). All error bars presented represent the standard errors of the performances of three membranes which were prepared under the same preparation condition. In addition, it has been proved that the effect of back-diffusion of $H_2$ on data analysis could be neglected.[37]

## Results and Discussion

### *Characterization of the PVAm–PIP films*

*Existing Form of PIP in the PVAm–PIP Film.* The possible intermolecular action between PIP and PVAm was investigated by ATR-FTIR and the spectra are displayed in

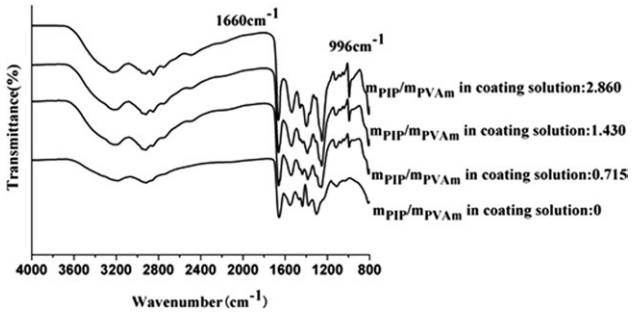


**Figure 3. ATR-FTIR spectra of PVAm–PIP films.**

Figure 3. It was found that, with the increase of $m_{PIP}/m_{PVAm}$ in the coating solution, the intensity of adsorption band around 996 $cm^{-1}$ assigned to the C—N stretching vibration, a characteristic band of PIP,[38,39] increases gradually, and the sharp characteristic band around 3200–3300 $cm^{-1}$, which represents the secondary amine group of PIP[40] does not appear. The above results show that there is no free PIP in the PVAm–PIP film. Therefore, it can be deduced that the PIP cross-links PVAm by the hydrogen bonds, because there are no chemical reaction between PVAm and PIP. Moreover, the lone pairs on the very electronegative oxygen atom of amide group or nitrogen atom of primary amine group in PVAm have strong intermolecular action with the slightly positive hydrogen atom of secondary amine group in PIP.[41] With the increase of $m_{PIP}/m_{PVAm}$ in the coating solution (from 0 to 2.860), the intensity of absorption band around 1660 $cm^{-1}$ which is assigned to the C=O stretching vibration (Amide I)[42] has no obvious changes. The result indicates that the hydrogen bonds cannot form between the secondary amine group of PIP and the amide group in PVAm.[20] According to ATR-FTIR study, it can be concluded that the intermolecular hydrogen bond in the PVAm–PIP film indeed formed between the secondary amine group of PIP and the primary amine group in PVAm.

As shown in Table 1, when the $m_{PIP}/m_{PVAm}$ in the coating solution is less than 1.430, the DRD of PIP in the PVAm–PIP film is higher than 90%, which shows that the PIP in the PVAm–PIP film is hardly volatile. When the $m_{PIP}/m_{PVAm}$ in the coating solution is 2.860, the DRD of PIP in the PVAm–PIP film is 80.4%. Hence, most of PIP is fixed in the PVAm–PIP film with different $m_{PIP}/m_{PVAm}$ in the coating solution.

Figure 4 shows that the HRD of PIP in the PVAm–PIP film decreases with increasing heat-treated temperature. No obvious weight loss of PIP in the PVAm–PIP film is observed with increasing heat-treated temperature from 30 to 80°C, indicating that PIP was fixed steadily in the PVAm–PIP film below 80°C. Even though the heat-treated temperature reaches 150°C, the HRD of PIP in the PVAm–PIP film

**Table 1. The $m_{PIP}/m_{PVAm}$ in the Coating Solutions and PVAm–PIP films**

| Coating Solution Composition | $m_{PIP}/m_{PVAm}$ in the Coating Solution | $m_{PIP}/m_{PVAm}$ in the Film | DRD (%) |
|---|---|---|---|
| 20 kg/$m^3$ PVAm 14.3 kg/$m^3$ PIP | 0.715 | 0.714 | 99.9 |
| 20 kg/$m^3$ PVAm 28.6 kg/$m^3$ PIP | 1.43 | 1.33 | 93 |
| 20 kg/$m^3$ PVAm 57.2 kg/$m^3$ PIP | 2.86 | 2.3 | 80.4 |

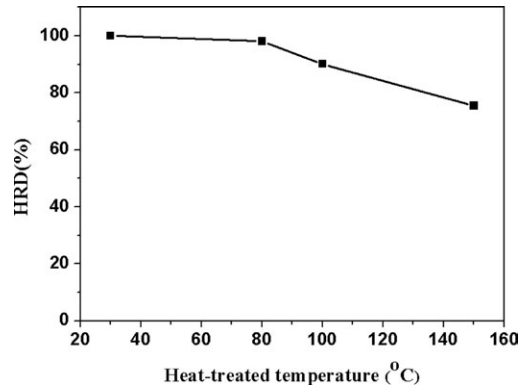


**Figure 4. HRD of PIP in the PVAm–PIP film with the variation of heat-treated temperature, $m_{PIP}/m_{PVAm}$ in the coating solution: 1.430.**

is as high as 75.5%. Therefore, most of PIP can be fixed in the film by the hydrogen bonds at 150°C.

According to ATR-FTIR and elemental analysis results, almost all the PIP is fixed steadily in the PVAm–PIP/PS composite membrane below 80°C by the intermolecular hydrogen bonds between the secondary amine group of PIP and the primary amine group in PVAm.

*Introducing Carrier Concentration by PIP Cross-linking PVAm in the PVAm–PIP Film.* The introducing PIP concentration by PIP cross-linking PVAm in the PVAm–PIP film was calculated by the $m_{PIP}/m_{PVAm}$ in the PVAm–PIP film dividing the molar mass of PIP. The introducing carrier concentration was two times as much as the introducing PIP concentration. Figure 5 shows the introducing carrier concentration by PIP cross-linking PVAm with different $m_{PIP}/m_{PVAm}$ in the PVAm–PIP coating solution. For comparison, the introducing carrier concentration by EDA cross-linking PVAm with different $m_{EDA}/m_{PVAm}$ in the PVAm–EDA coating solution[20] is also shown in Figure 5. As shown in Figure 5, with increasing $m_{PIP}/m_{PVAm}$ in the coating solution, the introducing carrier concentration by PIP cross-linking PVAm largely increases. The introducing carrier concentration by PIP cross-linking PVAm is much higher than that by EDA cross-linking PVAm. When the $m_{PIP}/m_{PVAm}$ in the coating solution is 2.860, the introducing carrier concentration by PIP cross-linking PVAm in the PVAm–PIP film is 53 mol/kg PVAm, which is 2.4 times of the largest introducing

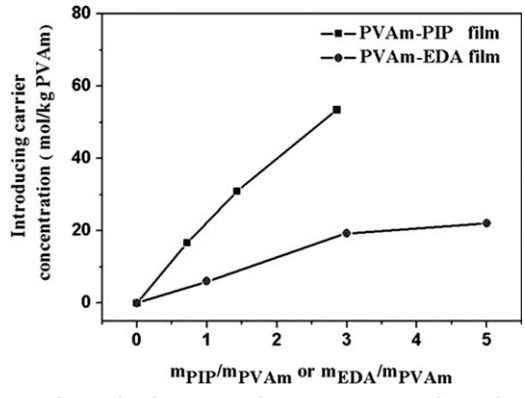


**Figure 5. Introducing carrier concentration by PIP cross-linking PVAm and EDA cross-linking PVAm.**

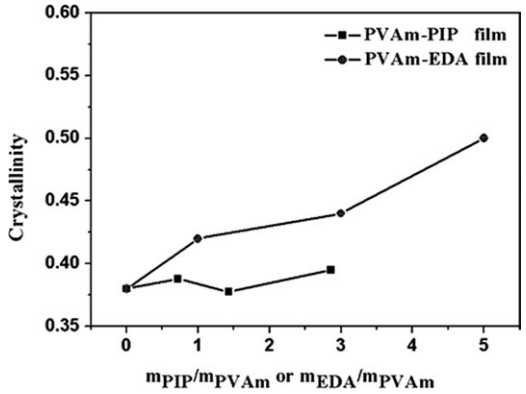


**Figure 6. Crystallinity of PVAm–PIP film and PVAm–EDA film.**

carrier concentration by EDA cross-linking PVAm of 22 mol/kg PVAm in the PVAm–EDA film.[20]

*Crystallinity of the PVAm–PIP Film.* Figure 6 shows the crystallinity of the PVAm–PIP film with different $m_{PIP}/m_{PVAm}$ in the PVAm–PIP coating solution. For comparison, the crystallinity of the PVAm–EDA film with different $m_{EDA}/m_{PVAm}$ in the PVAm–EDA coating solution[20] is also shown in Figure 6. As shown in Figure 6, when the $m_{PIP}/m_{PVAm}$ in the coating solution increases from 0.715 to 1.430, the crystallinity of the PVAm–PIP film slightly decreases, and when the $m_{PIP}/m_{PVAm}$ in the coating solution increases from 1.430 to 2.860, the crystallinity of the PVAm–PIP film slightly increases. However, compared with the crystallinity of the PVAm–EDA film, the crystallinity of the PVAm–PIP film is lower. The crystallinity of the PVAm–PIP film changes slightly with increasing $m_{PIP}/m_{PVAm}$ in the coating solution in comparison with that of the PVAm–EDA film. According to Sections of Introducing Carrier Concentration by PIP Cross-linking PVAm in the PVAm–PIP Film and Crystallinity of the PVAm–PIP film, due to the comprehensive effects of the introducing carrier concentration and the crystallinity, the effective carrier concentration of the PVAm–PIP/PS composite membrane is much higher than that of the PVAm–EDA/PS composite membrane, which is in favor of promoting the $CO_2$ facilitated transport. Therefore, the performance of the PVAm–PIP/PS composite membrane may greatly increase, which will be proved in the following section.

### *Performance of the PVAm–PIP/PS composite membrane*

*Effect of $m_{PIP}/m_{PVAm}$ in the Coating Solution on the Performance of the Membrane.* Figure 7 illustrates the $CO_2$ permeance, $N_2$ permeance, and $CO_2/N_2$ selectivity of the PVAm–PIP/PS composite membrane with different $m_{PIP}/m_{PVAm}$ in the coating solution at room-temperature (22°C). For comparison, Figure 7 also shows the $CO_2/N_2$ permselectivity of the PVAm–EDA/PS composite membrane with the $m_{EDA}/m_{PVAm}$ of 3 in the coating solution.[20] When the wet coating thicknesses of the membranes are all 200 $\mu$m, among the different $m_{EDA}/m_{PVAm}$ in the coating solution investigated in our previous work, the membrane with the $m_{EDA}/m_{PVAm}$ of 3 showed the highest performance.[20]

As shown in Figure 7, with increasing feed pressure, due to the tendency toward saturation of effective carriers,[43] the $CO_2$ permeance of the PVAm–PIP/PS composite membranes with 200 $\mu$m wet coating thickness and different $m_{PIP}/m_{PVAm}$ in the coating solution drops rapidly within the feed pressure range from 0.11 to 0.6 MPa, and then decreases gently within the higher pressure range from 0.6 to 1.6 MPa.

As shown in Figure 7a, when the $m_{PIP}/m_{PVAm}$ in the coating solution increases from 0.715 to 1.430, the $CO_2$ permeance increases rapidly, whereas the $CO_2$ permeance decreases rapidly when the $m_{PIP}/m_{PVAm}$ in the coating solution increases from 1.430 to 2.860. Among the different $m_{PIP}/m_{PVAm}$ in the coating solution investigated in this work, the membrane with the $m_{PIP}/m_{PVAm}$ of 1.430 showed the

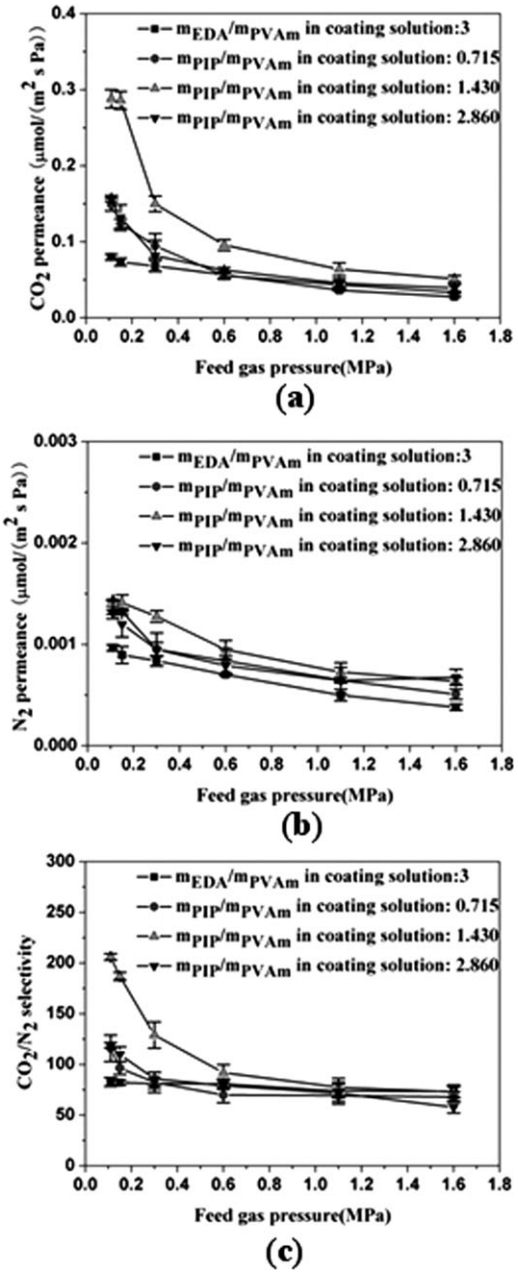


**Figure 7. The $CO_2/N_2$ separation performance of the PVAm–PIP/PS composite membrane with different $m_{PIP}/m_{PVAm}$ in the coating solution and the PVAm–EDA/PS composite membrane with the $m_{EDA}/m_{PVAm}$ of 3 in the coating solution: (a) $CO_2$ permeance; (b) $N_2$ permeance; (c) $CO_2/N_2$ selectivity.**

**Wet coating thickness: 200 $\mu$m. 22°C.**

highest $CO_2$ permeance. During the $CO_2$ separation process, the variation of $CO_2$ permeance with the $m_{PIP}/m_{PVAm}$ in the coating solution is attributed to the comprehensive effects of three factors.

1. With increasing $m_{PIP}/m_{PVAm}$ in the coating solution from 0.715 to 2.860, the increasing effective carrier concentration will result in the variation of the permeance of $CO_2$ ($CO_2$–carrier complex and uncomplexed $CO_2$). It can be explained as follows. The facilitated transport of $CO_2$ in the membranes containing primary or secondary amine groups was considered as the following formulas[33,44]

$$CO_2 + RR'NH \rightleftharpoons RR'NH^+COO^- \quad (3)$$

$$RR'NH^+COO^- + RR'NH \rightleftharpoons RR'NCOO^- + RR'NH_2^+ \quad (4)$$

$$RR'NH^+COO^- + H_2O \rightleftharpoons RR'NCOO^- + H_3O^+ \quad (5)$$

$$RR'NCOO^- + H_2O \rightleftharpoons RR'NH + HCO_3 \quad (6)$$

where R′ may be an H or another group. The reaction between $CO_2$ and amine carriers is defined as the zwitterions mechanism in formula (3)–(6). First, $CO_2$ reacts with primary or secondary amines to form zwitterions as an intermediate. Then, the zwitterions are deprotonated by amine or $H_2O$ to form the carbamate ion. The carbamate ions of the amine carrier are unstable and could react with $H_2O$ to form bicarbonate ions. From the formulas of (3)–(6), the amine carrier can react with $CO_2$ to form zwitterion, protonation-amine, carbamate ions, and bicarbonate ions. The $CO_2$ which follows facilitated transport is conveyed in the $CO_2$-carrier complex forms of carbamate and bicarbonate. With increasing $m_{PIP}/m_{PVAm}$ in the coating solution, on one hand, the concentration of effective carriers reacting with $CO_2$ increases rapidly in the membrane, which is favorable for $CO_2$ facilitated transport (see the section of characterization of the PVAm–PIP films) and will result in the great increase of the permeance of $CO_2$-carrier complex; on the other hand, the number of ions formed by reaction increases rapidly. Compared with quadrupole moment molecule $CO_2$, these ions have a stronger affinity to $H_2O$. Thus, the amount of water molecule which is used for dissolving $CO_2$ decreases, and the solubility of $CO_2$ in the water swelling membrane decreases,[45] which is called "salting-out" effect.[46] In addition, the diffusion of the carbamate and bicarbonate ions decreases with strengthening interaction of different ions, which weakens the facilitated transport of $CO_2$ in the membrane. Therefore, both the "salting-out" effect and ion interaction in the membrane which increase with increasing $m_{PIP}/m_{PVAm}$ in the coating solution will result in the decrease of the $CO_2$ permeance.

2. The variation of the crystallinity will result in the variation of the $CO_2$ permeance. When the $m_{PIP}/m_{PVAm}$ in the coating solution increases from 0.715 to 1.430, the crystallinity of the PVAm–PIP film slightly decreases (see Figure 6), which will result in the increase of the $CO_2$ permeance. When the $m_{PIP}/m_{PVAm}$ in the coating solution increases from 1.430 to 2.860, the crystallinity of the PVAm–PIP film slightly increases (see Figure 6), which will result in the decrease of the $CO_2$ permeance. However, during the $CO_2$ separation process, compared with the effective carrier concentration, the slight variation of the crystallinity affects the variation of the $CO_2$ permeance with different $m_{PIP}/m_{PVAm}$ in the coating solution more slightly.

3. The increasing densification of the selective layer will decrease the $CO_2$ permeance.[47] It can be explained as follows. The selective layer thickness of the membrane prepared by the coating solution with different $m_{PIP}/m_{PVAm}$ (from 0.715 to 2.860) and 200 $\mu$m wet coating thickness shows roughly around 0.78 $\mu$m according to SEM cross-section images, which indicates that the selective layer thickness is mainly dependent on the PVAm polymer content in the coating solution due to the small molecular volume of PIP and the densification of polymer matrix with addition of PIP. Hence, the amount of PIP added in the coating solution has no obvious effect on the selective layer thickness of the membrane, but it has obvious effect on the densification of polymer matrix by moderate hydrogen bond cross-linking which increases gradually with increasing $m_{PIP}/m_{PVAm}$ in the coating solution. In summary, the moderate hydrogen bond cross-linking leads to the increasing densification of the selective layer, which will decrease the $CO_2$ permeance.

As shown in Figure 7b, with increasing feed pressure from 0.11 to 1.6 MPa, $N_2$ permeance of the PVAm–PIP/PS composite membrane with different $m_{PIP}/m_{PVAm}$ in the coating solution declines continuously due to the membrane compaction which would decrease the amount of free volume and subsequently reduce the mobility of the penetrating molecules.[47] Figure 7b displays that, when the $m_{PIP}/m_{PVAm}$ in the coating solution increases from 0.715 to 1.430, $N_2$ permeance of PVAm–PIP/PS composite membranes slightly increases, and when the $m_{PIP}/m_{PVAm}$ in the coating solution increases from 1.430 to 2.860, $N_2$ permeance of PVAm–PIP/PS composite membranes decreases gently. $N_2$ transports through the membrane only following the solution-diffusion mechanism.[48] During the $CO_2$ separation process, the variation of $N_2$ permeance with increasing $m_{PIP}/m_{PVAm}$ in the coating solution is mainly attributed to the comprehensive effects of two factors. (1) The variation of the crystallinity will have an influence on $N_2$ permeance. When the $m_{PIP}/m_{PVAm}$ in the coating solution increases from 0.715 to 1.430, the crystallinity of the PVAm–PIP film slightly decreases (see Figure 6), which will result in the increase of $N_2$ permeance. When the $m_{PIP}/m_{PVAm}$ in the coating solution increases from 1.430 to 2.860, the crystallinity of the PVAm–PIP film slightly increases (see Figure 6), which will result in the decrease of $N_2$ permeance. (2) The increasing densification of the selective layer with increasing $m_{PIP}/m_{PVAm}$ in the coating solution will decrease the $N_2$ permeance.[47]

As shown in Figure 7c, among the different $m_{PIP}/m_{PVAm}$ in the coating solution investigated in this work, the membrane with the $m_{PIP}/m_{PVAm}$ of 1.430 showed the highest $CO_2/N_2$ selectivity due to the variation of $CO_2$ and $N_2$ permeance.

In summary, with increasing $m_{PIP}/m_{PVAm}$ in the coating solution, the variation of $CO_2$ permeance and $CO_2/N_2$ selectivity are mainly attributed to the variation of the effective carrier concentration, the variation of the crystallinity, and the densification of the membranes. Among the different $m_{PIP}/m_{PVAm}$ in the coating solution investigated in this work, the membrane with the $m_{PIP}/m_{PVAm}$ of 1.430 showed the highest $CO_2$ permeance and $CO_2/N_2$ selectivity.

The PVAm–PIP/PS composite membrane with the highest performance and the PVAm–EDA/PS composite membrane with the highest performance were compared. It can be seen from Figure 7a that the PVAm–PIP/PS composite membrane (with the $m_{EDA}/m_{PVAm}$ of 1.430 in the coating solution)

shows much higher $CO_2$ permeance than the PVAm–EDA/PS composite membrane (with the $m_{EDA}/m_{PVAm}$ of 3 in the coating solution). This phenomenon can be explained as follows. (1) According to the Sections of Introducing Carrier Concentration by PIP Cross-linking PVAm in the PVAm–PIP Film and Crystallinity of the PVAm–PIP Film, the effective carrier concentration of the PVAm–PIP/PS composite membrane with the $m_{PIP}/m_{PVAm}$ of 1.430 in the coating solution is much higher than that of the PVAm–EDA/PS composite membrane with the $m_{EDA}/m_{PVAm}$ of 3 in the coating solution; (2) the crystallinity of the PVAm–PIP/PS composite membrane with the $m_{PIP}/m_{PVAm}$ of 1.430 in the coating solution is lower than that of the PVAm–EDA/PS composite membrane with the $m_{EDA}/m_{PVAm}$ of 3 in the coating solution (see Figure 6). Because of the lower crystallinity of the PVAm–PIP/PS composite membrane, as shown in Figure 7b, the $N_2$ permeance of the PVAm–PIP/PS composite membrane with the $m_{PIP}/m_{PVAm}$ of 1.430 in the coating solution is higher than that of the PVAm–EDA/PS composite membrane with the $m_{EDA}/m_{PVAm}$ of 3 in the coating solution. Because of the variation of $CO_2$ and $N_2$ permeance, as shown in Figure 7c, the $CO_2/N_2$ selectivity of the PVAm–PIP/PS composite membrane with the $m_{PIP}/m_{PVAm}$ of 1.430 in the coating solution is higher than that of the PVAm–EDA/PS composite membrane with the $m_{EDA}/m_{PVAm}$ of 3 in the coating solution.

The $CO_2$ permeance of the PVAm–PIP/PS composite membrane with the $m_{PIP}/m_{PVAm}$ of 1.430 in the coating solution and 200 $\mu$m wet coating thickness is about 3.6 and 1.8 times of that of the PVAm–EDA/PS composite membrane with the $m_{EDA}/m_{PVAm}$ of 3 in the coating solution and 200 $\mu$m wet coating thickness at 0.11 and 1.6 MPa, respectively, and the corresponding $CO_2/N_2$ selectivity is about 2.5 and 1.0 times, respectively.

*Effect of wet coating thickness on the performance of the membrane*. To obtain a higher $CO_2/N_2$ separation performance, the ultrathin PVAm–PIP/PS composite membrane was prepared by reducing the thickness of the selective layer.[20] Figure 8 displays that the selective layer thicknesses of the PVAm–PIP/PS composite membrane prepared using the coating solution with the $m_{PIP}/m_{PVAm}$ of 1.430 and 30, 50, and 200 $\mu$m wet coating thicknesses are 0.135, 0.22, and 0.78 $\mu$m, respectively. With decreasing wet coating thickness, the selective layer thicknesses of the PVAm–PIP/PS composite membrane proportionally decrease.

Figure 9 summarizes the effects of wet coating thickness on $CO_2$, $N_2$ permeance, and $CO_2/N_2$ selectivity of the PVAm–PIP/PS composite membrane prepared using the coating solution with the $m_{PIP}/m_{PVAm}$ of 1.430 at room-temperature (22°C). As shown in Figure 9a, $CO_2$ permeance of the membrane with thinner wet coating thickness is obviously higher than that of the membrane with thicker wet coating thickness. The $CO_2$ permeance of the PVAm–PIP/PS composite membrane with 50 $\mu$m wet coating thickness is about 1.4 and 1.4 times of the $CO_2$ permeance of those with 200 $\mu$m wet coating thickness at 0.11 and 1.6 MPa, respectively. The $CO_2$ permeance of the PVAm–PIP/PS composite membrane with 30 $\mu$m wet coating thickness is about 5.2 and 10.2 times of those with 50 $\mu$m wet coating thickness at 0.11 and 1.6 MPa, respectively.

As shown in Figure 9b, $N_2$ permeance of the membrane with thinner wet coating thickness is obviously higher than that of the membrane with thicker wet coating thickness. $N_2$ permeance of the PVAm–PIP/PS composite membrane with the wet coating thicknesses of 50 and 200 $\mu$m decreases gradually within the feed pressure range from 0.11 to 1.6

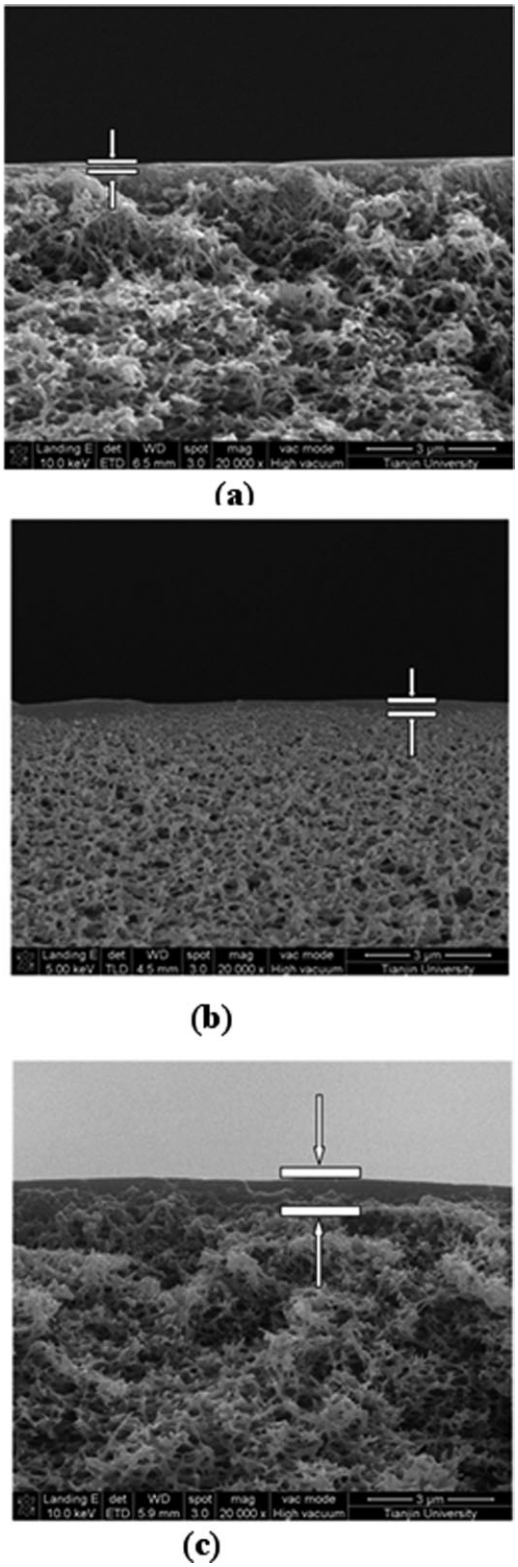


**Figure 8. SEM cross-sections of the PVAm–PIP/PS composite membrane prepared using coating solution with the $m_{PIP}/m_{PVAm}$ of 1.430: (a) 30 $\mu$m wet coating thickness; (b) 50 $\mu$m wet coating thickness; and (c) 200 $\mu$m wet coating thickness.**

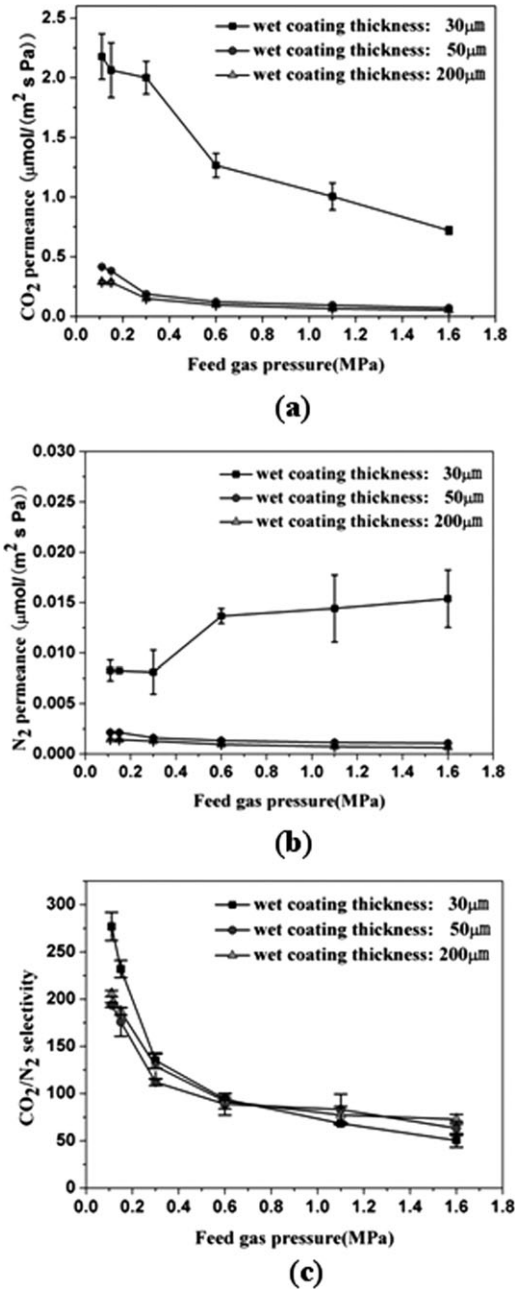


**Figure 9. Effects of wet coating thickness on the $CO_2$/$N_2$ permeance and selectivity of the PVAm–PIP/PS composite membrane prepared using coating solution with the $m_{PIP}/m_{PVAm}$ of 1.430: (a) $CO_2$ permeance; (b) $N_2$ permeance; and (c) $CO_2/N_2$ selectivity. 22°C.**

MPa. $N_2$ permeance of the PVAm–PIP/PS composite membrane with 30 $\mu$m wet coating thickness increases rapidly when the feed pressure is higher than 0.3 MPa. This is because with the reduction of the selective layer thickness, the glass transition temperature ($T_g$) of the selective layer decreases, and the mobility of the polymer chain increases.[49] In addition, when the feed pressure increases, the dissolved quantity of $CO_2$ in the polymer matrix increases, and thus, the intersegmental mobility in the polymer is enhanced.[50–52] Hence, the permeance of $N_2$ with 30 $\mu$m wet coating thickness increases rapidly at feed pressure exceeding 0.3 MPa.

Because of the variation of $CO_2$ and $N_2$ permeance mentioned above, as shown in Figure 9c, $CO_2/N_2$ selectivity of the PVAm–PIP/PS composite membranes has no obvious changes when the wet coating thickness decreases from 200 to 50 $\mu$m. However, the $CO_2/N_2$ selectivity of the PVAm–PIP/PS composite membrane with 30 $\mu$m wet coating thickness is about 1.4 and 0.8 times of those with 50 $\mu$m wet coating thickness at 0.11 and 1.6 MPa, respectively.

Table 2 presents the performance of the ultrathin PVAm–PIP/PS composite membrane with the $m_{PIP}/m_{PVAm}$ of 1.430 in the coating solution prepared in this work and other membranes with the maximal $CO_2$ permeance above 0.067 $\mu$mol/($m^2$ s Pa) reported in the literature.

As shown in Table 2, the PVAm–PIP/PS[a] and the PVAm–PIP/PS[b] composite membranes represent the ultrathin membranes prepared in this work with 30 $\mu$m and 50 $\mu$m wet coating thicknesses, respectively. The PVAm–PIP/PS[b] composite membrane shows much higher performance than the PVAm–EDA/PS composite membrane which has the same wet coating thickness with the PVAm–PIP/PS[b] composite membrane. As shown in Table 2, the $CO_2$ permeance of the PVAm–PIP/PS[b] composite membrane is about 2.0 and 1.6 times of that of the PVAm–EDA/PS composite membrane at 0.11 and 1.6 MPa, respectively, and the corresponding $CO_2/N_2$ selectivity is about 1.8 and 3.2 times, respectively. The $CO_2$ permeance of the PVAm–PIP/PS[a] composite membrane is about 10.7 and 16.8 times of that of the PVAm–EDA/PS composite membrane mentioned above at 0.11 and 1.6 MPa, respectively, and the corresponding $CO_2/N_2$ selectivity is about 2.6 and 2.5 times, respectively.

From Table 2 and Figure 9, it can be deduced that the $CO_2$ permeance of the PVAm–PIP/PS[a] composite membrane is about 30.7 and 68.3 times of that of the PVAm/PVA composite membrane presented in Table 2 at $CO_2$ partial pressure of 0.02 and 0.10 MPa, respectively, and the corresponding $CO_2/N_2$ selectivity is about 1.6 and 1.1 times, respectively. The $CO_2$ permeance of the PVAm–PIP/PS[b] composite membrane is about 5.9 and 6.5 times of that of the PVAm/PVA composite membrane mentioned above at $CO_2$ partial pressure of 0.02 and 0.10 MPa, respectively, and the corresponding $CO_2/N_2$ selectivity is about 1.1 and 1.1 times, respectively.

From Table 2 and Figure 9, it can be deduced that the $CO_2$ permeance of the PVAm–PIP/PS[a] composite membrane is about 6.6 and 5.8 times of that of the Polaris™ membrane at $CO_2$ partial pressure of 0.014 and 0.065 MPa, respectively, and the corresponding $CO_2/N_2$ selectivity is about 6.0 and 2.3 times, respectively. The $CO_2$ permeance of the PVAm–PIP/PS[b] composite membrane is about 1.3 and 0.5 times of that of the Polaris™ membrane mentioned above at $CO_2$ partial pressure of 0.014 and 0.065 MPa, respectively, and the corresponding $CO_2/N_2$ selectivity is about 4.1 and 2.0 times, respectively.

From Table 2 and Figure 9, it can be deduced that the $CO_2$ permeance of the PVAm–PIP/PS[a] composite membrane is about 5.0 and 3.9 times of that of the poly(ethylene oxide) (PEO)–poly(butylene terephthalate) (PBT)/polyethylene glycol (PEG)–dibutyl ether (DBE)(polyacrylonitrile (PAN)–poly(dimethylsiloxane) (PDMS)) membrane presented in Table 2 at $CO_2$ partial pressure of 0.14 and 0.28 MPa, respectively, and the corresponding $CO_2/N_2$ selectivity is about 2.2 and 1.8 times, respectively. The $CO_2$ permeance of the PVAm–PIP/PS[b] composite membrane is about 0.6 and 0.4 times of

**Table 2. Performance Comparison of the Membrane Obtained in This Work with Other Membranes**

| Membrane | Feed Gas ($CO_2$ vol %) | $R_{CO_2}$ ($\mu$mol/(m$^2$ s Pa)) | $\alpha$ | Permeate Side | $P_{CO_2}$ ($P$) | Reference |
|---|---|---|---|---|---|---|
| PVAm–PIP/PS[a] | $CO_2/N_2$ (20%) | 2.1775 | 277 | 0.1 MPa, $H_2$ as sweeping gas | 0.02 (0.11) | This work |
| | | 1.99995 | 135 | | 0.06 (0.3) | |
| | | 1.2663 | 94.1 | | 0.12 (0.6) | |
| | | 0.72025 | 50.5 | | 0.32 (1.6) | |
| PVAm–PIP/PS[b] | $CO_2/N_2$ (20%) | 0.4154 | 194 | 0.1 MPa, $H_2$ as sweeping gas | 0.02 (0.11) | This work |
| | | 0.187265 | 112 | | 0.06 (0.3) | |
| | | 0.121605 | 89 | | 0.12 (0.6) | |
| | | 0.070685 | 63 | | 0.32 (1.6) | |
| PVAm–EDA/PS | $CO_2/N_2$ (20%) | 0.203345 | 106 | 0.1 MPa, $H_2$ as sweeping gas | 0.02 (0.11) | 20 |
| | | 0.100165 | 63 | | 0.12 (0.6) | |
| | | 0.05829 | 35 | | 0.22 (1.1) | |
| | | 0.04288 | 20 | | 0.32 (1.6) | |
| PVAm/PVA | $CO_2/N_2$ (10%) | 0.07102 | 174 | 0.1 MPa, He as sweeping gas | 0.02 (0.2) | 31 |
| | | 0.02211 | 100 | | 0.10 (1.0) | |
| Polaris™ | $CO_2/N_2$ | 0.335 | 50 | 0.022 MPa | 0.014(0.11) | 18 |
| | | 0.335 | 50 | 0.1 MPa | 0.065(0.5) | |
| PEO–PBT/PEG-DBE (PAN–PDMS) | $CO_2/N_2$ (28%) | 0.24455 | 40 | 0.11 MPa, no sweeping gas | 0.14 (0.5) | 13 |
| | | 0.211218 | 33 | | 0.28 (1.0) | |
| PEO–PBT (PAN–PDMS) | $CO_2/N_2$ (15%) | 0.30016 | 55 | 0.11 MPa, no sweeping gas | 0.09 (0.6) | 14 |
| | | 0.284315 | 47 | | 0.3 (2.0) | |

$P_{CO_2}$—$CO_2$ partial pressure of the feed gas (MPa); $P$—feed gas pressure (MPa). The prepared conditions of PVAm–PIP/PS composite membrane: the $m_{PIP}/m_{PVAm}$ in the coating solution is 1.430; the wet coating thickness of the PVAm–PIP/PS[a] composite membrane is 30 $\mu$m; the wet coating thickness of the PVAm–PIP/PS[b] composite membranes is 50 $\mu$m. The prepared condition of PVAm–EDA/PS composite membrane: the $m_{EDA}/m_{PVAm}$ in the coating solution is 3; wet coating thickness is 50 $\mu$m.

that of the PEO–PBT/PEG–DBE(PAN–PDMS) membrane mentioned above at $CO_2$ partial pressure of 0.14 and 0.28 MPa, respectively, and the corresponding $CO_2/N_2$ selectivity is about 2.2 and 2.1 times, respectively.

From Table 2 and Figure 9, it can be deduced that the $CO_2$ permeance of the PVAm–PIP/PS[a] composite membrane is about 5.4 and 2.9 times of that of the PEO–PBT(PAN–PDMS) membrane at $CO_2$ partial pressure of 0.09 and 0.3 MPa, respectively, and the corresponding $CO_2/N_2$ selectivity is about 2.1 and 1.2 times, respectively. The $CO_2$ permeance of the PVAm–PIP/PS[b] composite membrane is about 0.5 and 0.3 times of that of the PEO–PBT(PAN–PDMS) membrane mentioned above at $CO_2$ partial pressure of 0.09 and 0.3 MPa, respectively, and the corresponding $CO_2/N_2$ selectivity is about 1.8 and 1.4 times, respectively.

In summary, the ultrathin membrane prepared in this work, especially the PVAm–PIP/PS[a] composite membrane, shows much higher $CO_2$ permeance and $CO_2/N_2$ selectivity compared with other membranes.

*Performance Stability of the PVAm–PIP/PS Composite Membrane*. As mentioned above, for the $CO_2/N_2$ separation membrane, $CO_2$ capture from flue gas is an important application. The temperature of the true operating flue gas is about 40–50°C in a real plant.[36] Therefore, the effect of the temperature on the performance of the PVAm–PIP/PS[b] composite membrane was investigated. As shown in Figure 10, compared with the membrane tested at 22°C, the performance of the membrane tested at 50°C has no obvious change.

The separation performance stability of the PVAm–PIP/PS[b] composite membrane was investigated at room-temperature (22°C) and 50°C. The membrane was tested continuously for 300 h using $CO_2/N_2$ mixed gas (20/80 by volume) at 0.15 MPa feed pressure at room-temperature (22°C). Then, a new PVAm–PIP/PS[b] composite membrane was tested continuously for 600 h using $CO_2/N_2$ mixed gas (20/80 by volume) at 0.15 MPa feed pressure at 50°C.

As shown in Figures 11 and 12, the separation performance of the PVAm–PIP/PS[b] composite membrane is fairly stable with the humidified feed gas. As shown in Figure 11, when the humidification is discontinued, sudden decrease of both $CO_2$ permeance and $CO_2/N_2$ selectivity is observed due to the loss of water which not only weakens the $CO_2$ facilitated transport but also makes the membrane become rigid without swelling effect.[48] When the feed gas is humidified again, the separation performance of the membrane is quickly well recovered. Figures 11 and 12 indicate that during the $CO_2$ separation process, the PIP is fixed steadily in the PVAm–PIP/PS composite membrane.

$O_2$, $SO_2$, $NO_x$ (NO and $NO_2$) gas which are present in the flue gas may have effects on the performance stability of the PVAm–PIP/PS composite membrane prepared in this work. According to the literature,[53] in the flue gas, the amount of $O_2$ is about 5%, the amount of $SO_2$ is about 200 ppm, and the amount of $NO_x$ is less than 50 ppm. A method has been used widely to evaluate the chlorine resistance of the reverse osmosis membrane, by testing the changes in the separation performance of the membrane before and after a short time to exposure an aqueous solution with a high concentration of free chlorine.[54,55] With a similar method, the effects of $O_2$, $SO_2$, $NO_x$ ($NO_2$ and NO) gases in the flue gas saturated with water vapor on the performance of the PVAm–PIP/PS composite membrane was evaluated by testing the changes in the separation performance of the PVAm–PIP/PS[b] composite membrane before and after exposure to pure $O_2$, $SO_2/CO_2/N_2$ (2/18/80 by volume) mixed gas, $NO_2/NO/CO_2/N_2$ (1/1/18/80 by volume) mixed gas saturated with water vapor for 200, 120, and 30 h, respectively, which can be considered as being equal to the membrane before and after exposure to $O_2/CO_2/N_2$ (5/15/80 by volume), $SO_2/CO_2/N_2$ (0.02/19.98/80 by volume), $NO_2/NO/CO_2/N_2$ (0.0025/0.0025/19.995/80 by volume) mixed gases saturated with water vapor for 4000, 12,000, and 12,000 h, respectively.[54]

As shown in Figures 13–15, after the membrane was exposed to $H_2O$-saturated pure $O_2$, $SO_2/CO_2/N_2$ mixed gas, and $NO_2/NO/CO_2/N_2$ mixed gas for a certain time, respectively, the $CO_2/N_2$ separation performance of the membrane showed a recovery process. At the beginning, the $CO_2$ permeance and $CO_2/N_2$ selectivity were lower and then

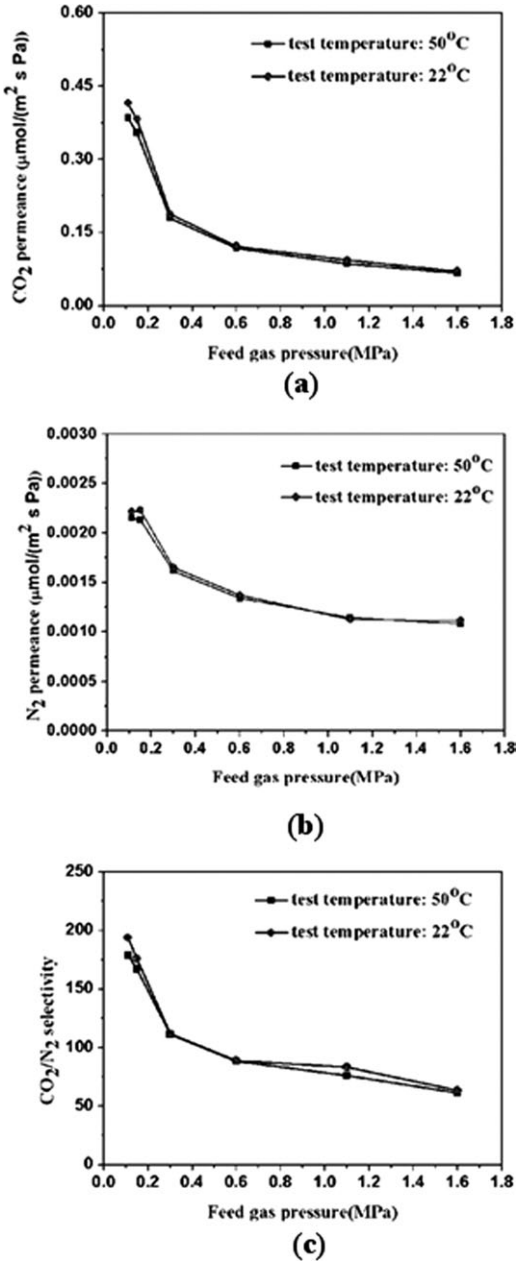


**Figure 10. Effects of the temperature on the $CO_2/N_2$ permeance and selectivity of the PVAm–PIP/PS composite membrane prepared using coating solution with the $m_{PIP}/m_{PVAm}$ of 1.430 and 50 $\mu$m wet coating thickness: (a) $CO_2$ permeance; (b) $N_2$ permeance; and (c) $CO_2/N_2$ selectivity.**

increased with testing time. After about 1 h, the $CO_2$ permeance and $CO_2/N_2$ selectivity became stable, and the stable values were equal to that of the membrane before exposure to $H_2O$-saturated pure $O_2$, $SO_2/CO_2/N_2$ mixed gas, and $NO_2/NO/CO_2/N_2$ mixed gas (see Figure 9). Clearly, of course, real flue gases will contain these problematic contaminants, so the actual performance of the membrane reported here under idealized humidified simple $CO_2/N_2$ feed conditions with humidified downstream sweep conditions, vs. the performance of the membrane under actual use conditions, will be greatly overestimated.

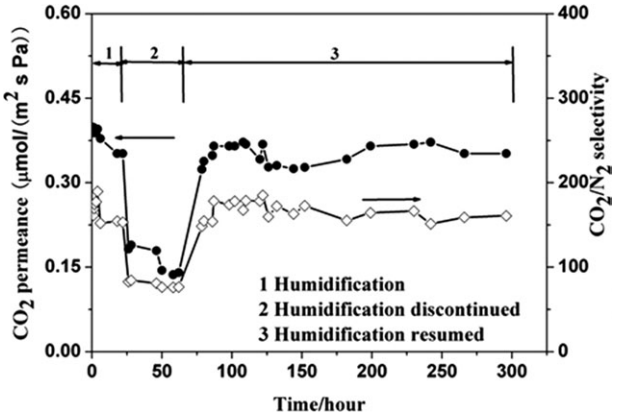


**Figure 11. Separation performance stability of the PVAm–PIP/PS composite membrane prepared using coating solution with the $m_{PIP}/m_{PVAm}$ of 1.430 and 50 $\mu$m wet coating thickness. Feed gas: 20 vol % $CO_2$ and 80 vol % $N_2$, 0.15 MPa. 22°C.**

Moreover, the PVAm–PIP/PS[b] composite membrane was tested by $O_2/CO_2/N_2$ (2/18/80 by volume), $SO_2/CO_2/N_2$ (2/18/80 by volume), $NO_2/NO/CO_2/N_2$ (1/1/18/80 by volume) mixed gases saturated with water vapor. As shown in Figures 16–18, both the $CO_2$ permeance and $CO_2/N_2$ selectivity of the PVAm–PIP/PS[b] composite membrane were lower than those of the membrane tested by $CO_2/N_2$ mixed gas (see Figure 9). However, the $CO_2$ permeance and $CO_2/N_2$ selectivity of the membrane were stable with time.

The above results show that $O_2$, $SO_2$, $NO_x$ absorptions in the membrane cause the decrease of membrane performance. It may be attributed to two factors. (1) $O_2$, $SO_2$, and $NO_x$ occupy a part of carriers, which restrains the reaction between $CO_2$ and the carriers. (2) $O_2$, $SO_2$, and $NO_x$ occupy a part of the transport channels of $CO_2$, which also restrains the $CO_2$ transport in the membrane. With desorptions of the $O_2$, $SO_2$, $NO_x$ in the membrane, the membrane performance recoveries. Hence, it can be deduced that the absorptions of $O_2$, $SO_2$, and $NO_x$ in the membrane are reversible, and no

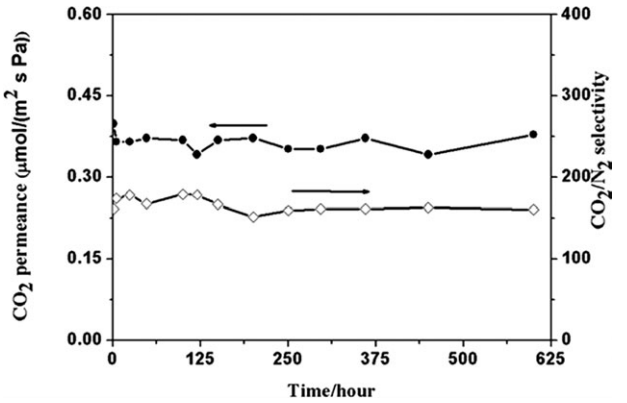


**Figure 12. Separation performance stability of the PVAm–PIP/PS composite membrane prepared using coating solution with the $m_{PIP}/m_{PVAm}$ of 1.430 and 50 $\mu$m wet coating thickness.**

**Feed gas: 20 vol % $CO_2$ and 80 vol % $N_2$, 0.15 MPa. 50°C.**

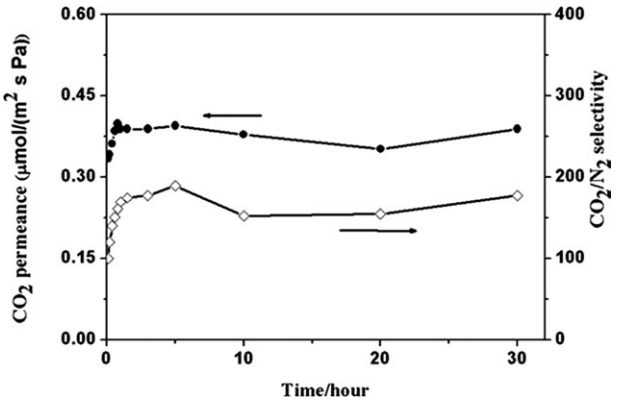


**Figure 13. The recovery process of $CO_2$ permeance and $CO_2/N_2$ selectivity of the PVAm–PIP/PS composite membrane after exposure to pure $O_2$ saturated with water vapor for 200 h.**

**The $m_{PIP}/m_{PVAm}$ in the coating solution: 1.430. Wet coating thickness: 50 μm. Feed gas: 20 vol % $CO_2$ and 80 vol % $N_2$, 0.15 MPa. 50°C.**

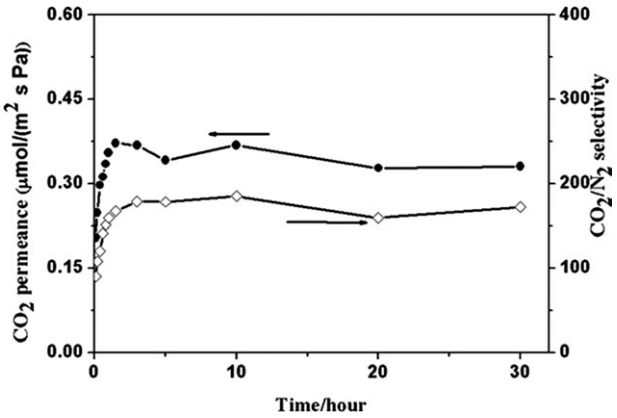


**Figure 15. The recovery process of $CO_2$ permeance and $CO_2/N_2$ selectivity of the PVAm–PIP/PS composite membrane after exposure to NO/$NO_2$/$CO_2$/$N_2$ (1/1/18/80 by volume) mixed gas saturated with water vapor for 30 h.**

**The $m_{PIP}/m_{PVAm}$ in the coating solution: 1.430. Wet coating thickness: 50 μm. Feed gas: 20 vol % $CO_2$ and 80 vol % $N_2$, 0.15 MPa. 50°C.**

obvious degradation of the membrane appears after the membrane is exposed to $H_2O$-saturated $CO_2/N_2$ mixed gas containing $O_2$, $SO_2$, and $NO_x$.

*Economic Evaluation of the PVAm–PIP/PS Composite Membrane*. The membrane prepared in our work is the flat sheet membrane, and the membrane is used to prepare the spiral wound membrane module. According to the literatures[11,12] and the market price, the cost of the membrane and membrane frame are estimated as follows. The flat sheet membrane cost is divided into four parts: the cost of the membrane materials (mainly PVAm and PIP) is \$37/m$^2$, the cost of the labor is \$33/m$^2$, the depreciation cost of the devices to prepare the membrane is \$5/m$^2$, and other cost is \$5/m$^2$. Hence, the flat sheet membrane cost should be \$80/m$^2$. The cost of spiral wound membrane frame is assumed to be \$394,000/2000 m$^2$. According to the method proposed by our previous works,[11,56] the economic evaluation of the PVAm–PIP/PS[a] composite membrane used for $CO_2$ capture was carried out. The $CO_2/N_2$ selectivity of the membrane mentioned above is not higher than 300, which cannot meet the requirement of the single-stage membrane system.[11] For the feed rate of 35 MMSCFD (11.57 m$^3$(standard temperature and pressure (STP)) s$^{-1}$) (20 vol % $CO_2$ + 80 vol % $N_2$), the separation target of product $CO_2$ purity > 95% and $CO_2$ recovery > 90% can be fulfilled by the two-stage membrane system.[11] Figure 19 is the two-stage membrane process with the feed compression.

As mentioned above, even if the performance of the membrane tested in the laboratory may be higher than that tested in the actual use, the performance of the membrane tested in the laboratory is still used to roughly carry out the economic evaluation in this work. Table 3 shows the performance and

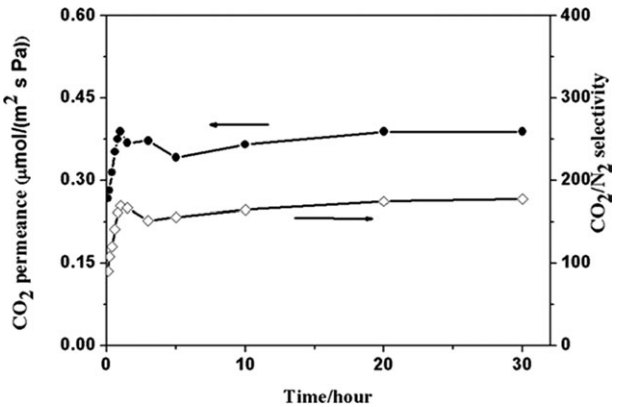


**Figure 14. The recovery process of $CO_2$ permeance and $CO_2/N_2$ selectivity of the PVAm–PIP/PS composite membrane after exposure to $SO_2$/$CO_2$/$N_2$ (2/18/80 by volume) mixed gas saturated with water vapor for 120 h.**

**The $m_{PIP}/m_{PVAm}$ in the coating solution: 1.430. Wet coating thickness: 50 μm. Feed gas: 20 vol % $CO_2$ and 80 vol % $N_2$, 0.15 MPa. 50°C.**

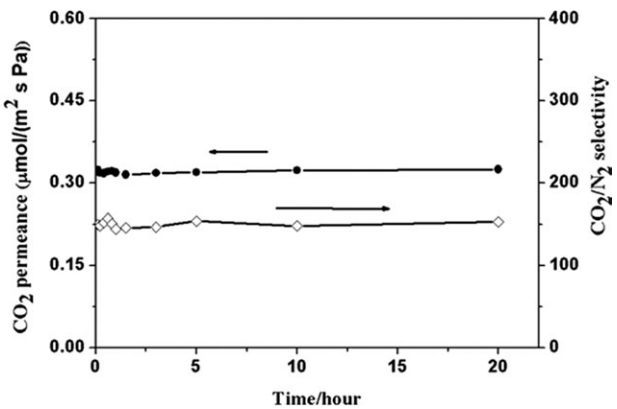


**Figure 16. Separation performance stability of the PVAm–PIP/PS composite membrane prepared using coating solution with the $m_{PIP}/m_{PVAm}$ of 1.430 and 50 μm wet coating thickness.**

**Feed gas: 2 vol % $O_2$, 18 vol %$CO_2$, and 80 vol %$N_2$, 0.15 MPa. 50°C.**

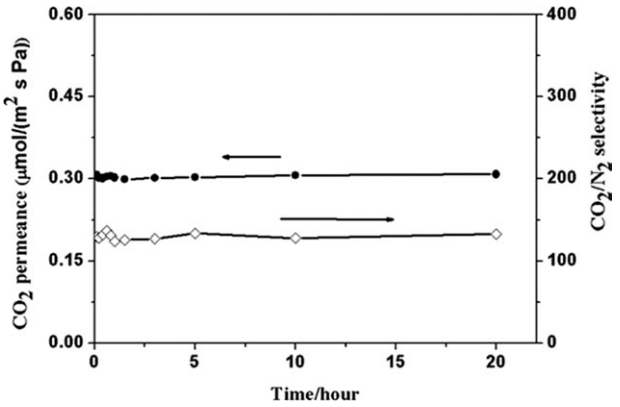


**Figure 17. Separation performance stability of the PVAm–PIP/PS composite membrane prepared using coating solution with the $m_{PIP}/m_{PVAm}$ of 1.430 and 50 $\mu$m wet coating thickness.**

**Feed gas: 2 vol % $SO_2$, 18 vol %$CO_2$, and 80 vol %$N_2$, 0.15 MPa. 50°C.**

the cost of the two-stage membrane process with the feed compression.

As the cost of the traditional chemical absorption method is about \$45–80/1000 kg $CO_2$ recovered,[12] the results in Table 3 show that, compared with the chemical absorption method, the cost of case 1–3 has an obvious superiority, which means that the membrane prepared in this work has a bright future in the industrial application of $CO_2$ capture.

## Conclusions

In this work, the PVAm–PIP/PS composite membrane prepared by coating the PVAm–PIP mixed aqueous solution on the PS ultrafiltration membrane showed high $CO_2/N_2$ separation performance. Some conclusions were obtained as follows.

1. The results of ATR-FTIR and elemental analyses indicated that almost all the PIP was fixed steadily in the PVAm–PIP/PS composite membrane below 80°C by the intermolecular hydrogen bonds between secondary amine group of PIP and primary amine group in PVAm. The results of elemental and XRD analyses showed that PIP as the cross-linking agent can largely improve the effective carrier concentration in the PVAm–PIP/PS composite membrane.

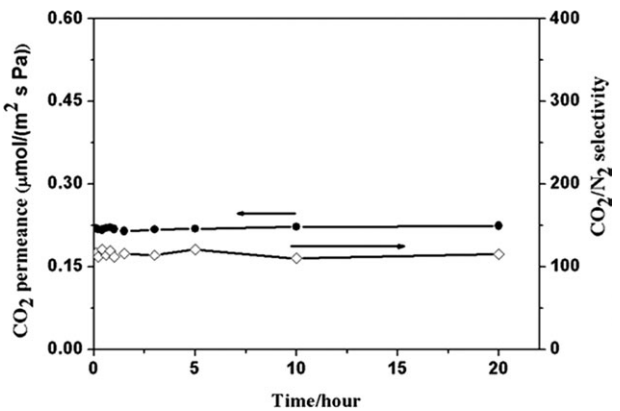


**Figure 18. Separation performance stability of the PVAm–PIP/PS composite membrane prepared using coating solution with the $m_{PIP}/m_{PVAm}$ of 1.430 and 50 $\mu$m wet coating thickness.**

**Feed gas: 1 vol % $NO_2$, 1 vol % NO, 18 vol %$CO_2$ and 80 vol %$N_2$, 0.15 MPa. 50°C.**

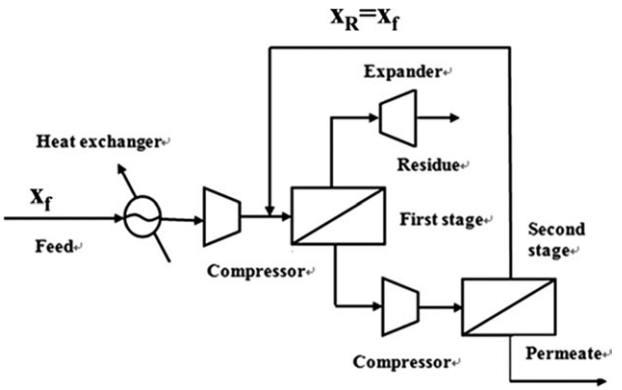


**Figure 19. Schematic diagram of two-stage membrane process with recycle (feed compression).[11]**

**$X_f$ = $CO_2$ mole fraction of the feed gas, $X_R$ = the recycle $CO_2$ mole fraction.**

2. Ultrathin PVAm–PIP/PS composite membranes were prepared. Using $CO_2/N_2$ mixed gas (20/80 by volume) as the feed gas, the membrane with the $m_{PIP}/m_{PVAm}$ of 1.430 in the coating solution and 30 $\mu$m wet coating thickness showed $CO_2$ permeance of 2.1775 and 0.72025 $\mu$mol/(m$^2$ s Pa) at feed pressure of 0.11 and 1.6 MPa, respectively, and the corresponding $CO_2/N_2$ selectivity of 277 and 50.5, respectively.

3. The separation performance stability of the PVAm–PIP/PS composite membrane with the $m_{PIP}/m_{PVAm}$ of 1.430 in the coating solution and 50 $\mu$m wet coating thickness was tested using $CO_2/N_2$ mixed gas (20/80 by volume) for 300 h at 0.15 MPa feed pressure. No obvious deterioration of $CO_2$ permeance and $CO_2/N_2$ selectivity was observed.

4. The ultrathin membrane prepared in this work, especially the PVAm–PIP/PS[a] composite membrane, showed much higher $CO_2$ permeance and $CO_2/N_2$ selectivity than other membranes reported in the literature. For $CO_2$ capture, the two-stage membrane system using the PVAm–PIP/PS[a] composite membrane has a cost-superiority in comparison

**Table 3. Performance of the Membrane Process with Feed Compression***

| Case | 1 | 2 | 3 |
|---|---|---|---|
| Membrane selectivity | 94.1 | 68.4 | 50.5 |
| $CO_2$ permeance ($\mu$mol/(m$^2$ s Pa)) | 1.2663 | 1.005 | 0.72025 |
| Feed pressure (MPa) | 0.6 | 1.1 | 1.6 |
| Permeate pressure(MPa) | 0.1 | 0.1 | 0.1 |
| Pressure ratio | 0.167 | 0.091 | 0.0625 |
| Membrane area ($10^4$ m$^2$) | 2.14 | 0.44 | 0.25 |
| $CO_2$ recovery (vol %) | 90.3 | 90.2 | 90.2 |
| Product purity (vol %) | 95.8 | 97.6 | 97.5 |
| Recycle flow rate (m$^3$ (STP) s$^{-1}$) | 1.72 | 1.59 | 1.25 |
| Energy [MJ/(kg $CO_2$ recovered)] | 1.29 | 1.66 | 1.99 |
| Total cost (\$/1000 kg $CO_2$ recovered) | 26.4 | 28.5 | 32.9 |

*The membrane is the PVAm–PIP/PS[a] composite membrane, that is, the $m_{PIP}/m_{PVAm}$ in the coating solution is 1.430, and the wet coating thickness of the PVAm–PIP/PS[a] composite membrane is 30 $\mu$m. In this membrane process, according to the cost of the materials, labor and the depreciation, and so forth, the membrane cost is assumed to be \$80/m$^2$, membrane frame cost is assumed to be \$394,000/2000 m$^2$.[11,12] Operation temperature is 25°C, operation time is 5 years and 8000 h/year, the average electricity fee is assumed to be \$0.0531/Kwh,[11,12] and feed rate is 35 MMSCFD (11.57 m$^3$(STP)/s).[11]

with the traditional chemical absorption method. For example, at 0.6 MPa feed pressure and 0.1 MPa permeate pressure, the cost of the two-stage membrane system using the PVAm–PIP/PS[a] composite membrane is \$26.4/1000 kg $CO_2$ recovered, and at 1.1 MPa feed pressure and 0.1 MPa permeate pressure, the cost of the two-stage membrane system using the PVAm–PIP/PS[a] composite membrane is \$28.5/1000 kg $CO_2$ recovered.

## Acknowledgments

This research is supported by the Natural Science Foundation of China (No. 20836006), the National Basic Research Program (No. 2009CB623405), the Science & Technology Pillar Program of Tianjin (No. 10ZCKFSH01700), the Programme of Introducing Talents of Discipline to Universities (No. B06006), and the Cheung Kong Scholar Program for Innovative Teams of the Ministry of Education (No. IRT0641).

## Notation

$R_{CO_2}$ = the $CO_2$ permeance, $\mu$mol/(m$^2$ s Pa)
$\alpha$ = the $CO_2/N_2$ selectivity
$P_{CO_2}$ = the $CO_2$ partial pressure of the feed gas, MPa
$P$ = the feed gas pressure, MPa

## Literature Cited

1. Lin HQ, Freeman BD. Materials selection guidelines for membranes that remove $CO_2$ from gas mixtures. *J Mol Struct*. 2005; 739:57–74.
2. Baker RW. Future directions of membrane gas separation technology. *Ind Eng Chem Res*. 2002;41:1393–1411.
3. Sonny S, Anil K. Separation of dyes using composite carbon membranes. *AIChE J*. 2009;55:1712–1722.
4. Ho MT, Allison GW, Wiley DE. Reducing the cost of $CO_2$ capture from flue gases using membrane technology. *Ind Eng Chem Res*. 2008;47:1562–1568.
5. Jiang LY, Chen HM, Jean YC, Chung TS. Ultrathin polymeric Interpenetration network with separation performance approaching ceramic membranes for biofuel. *AIChE J*. 2009;55:75–86.
6. Strathmann H. Membrane separation processes: current relevance and future opportunities. *AIChE J*. 2001;47:1077–1087.
7. Favre E. Carbon dioxide recovery from post-combustion processes: can gas permeation membranes compete with absorption? *J Membr Sci*. 2007;294:50–59.
8. Zhao L, Riensche E, Menzer R, Blum L, Stolten D. A parametric study of $CO_2/N_2$ gas separation membrane processes for post-combustion capture. *J Membr Sci*. 2008;325:284–294.
9. Zhao L, Riensche E, Blum L, Stolten D. Multi-stage gas separation membrane processes used in post-combustion capture: Energetic and economic analyses. *J Membr Sci*. 2010;359:160–172.
10. Hussain A, Hägg MB. A feasibility study of $CO_2$ capture from flue gas by a facilitated transport membrane. *J Membr Sci*. 2010;359: 140–148.
11. Yang DX, Wang Z, Wang JX, Wang SC. Potential of two-stage membrane system with recycle stream for $CO_2$ capture from post-combustion gas. *Energy Fuels*. 2009;23:4755–4762.
12. Zhao L, Menzer R, Riensche E, Blum L, Stolten D. Concepts and investment cost analyses of multi-stage membrane systems used in post-combustion processes. *Energy Procedia. GHGT 9*. 2009;1:269–278.
13. Yave W, Car A, Funari SS, Nunes SP, Peinemann KV. $CO_2$-philic polymer membrane with extremely high separation performance. *Macromolecules*. 2010;43:326–333.
14. Yave W, Car A, Wind J, Peinemann KV. Nanometric thin film membranes manufactured on square meter scale: ultra-thin films for $CO_2$ capture. *Nanotechnology*. 2010;21:395301.1–395301.7.
15. Car A, Stropnik C, Yave W, Peinemann KV. PEG modified poly (amide-bethylene oxide) membranes for $CO_2$ separation. *J Membr Sci*. 2008;307:88–95.
16. Car A, Stropnik C, Yave W, Peinemann KV. Tailor-made polymeric membranes based on segmented block copolymers for $CO_2$ separation. *Adv Funct Mater*. 2008;23:2815–2823.
17. Yave W, Car A, Peinemann KV. Nanostructured membrane material designed for carbon dioxide separation. *J Membr Sci*. 2010;350:124–129.
18. Merkel TC, Lin HQ, Wei XT, Baker R. Power plant post-combustion dioxide capture: an opportunity for membranes. *J Membr Sci*. 2010;359:126–139.
19. Lin HQ, Freeman BD. Gas and vapor solubility in cross-linked poly(ethylene glycol diacrylate). *Macromolecules*. 2005;38:8394–8407.
20. Yuan SJ, Wang Z, Qiao ZH, Wang MM, Wang JX, Wang SC. Improvement of $CO_2/N_2$ separation characteristics of polyvinylamine by modifying with ethylenediamine. *J Membr Sci*. 2011;378:425–437.
21. Paul DR, Yampol'skii YP. *Polymeric Gas Separation Membranes*. Boca Raton, FL: CRC, 1994.
22. Mulder M. *Basic Principles of Membrane Technology*, 2nd ed. Dordrecht, The Netherlands: Kluwer Academic Publishers, 1999.
23. Kanehashi SJ, Kusakabe A, Sato SC, Nagai K. Analysis of permeability; solubility and diffusivity of carbon dioxide, oxygen, and nitrogen in crystalline and liquid crystalline polymers. *J Membr Sci*. 2010;365:40–51.
24. Yi CH, Wang Z, Li M, Wang JX, Wang SC. Facilitated transport of $CO_2$ through polyvinylamine/polyethylene glycol blend membranes. *Desalination*. 2006;193:90–96.
25. Zhen HF, Wang Z, Li BA, Wang SC. A review of polymeric membrane for carbon dioxide separation. *Polym Mater Sci Technol. [in Chinese]*. 1999;15:29–31.
26. Wang Z, Lu Q, Li BA, Wang SC. Structure and performance of a new composite membrane used for $CO_2$ separation. *Polym Mater Sci Eng. [in Chinese]*. 2000;16:5–7.
27. Zhen HF, Wang Z, Li BA, Ren Y, Wang SC. Gas sorptive property of novel membrane used for $CO_2$ separation. *J Chem Ind Eng. [in Chinese]*. 2000;51:823–826.
28. Wang Z, Dong CM, Lu Q, Wang SC. Preparation and $CO_2$ separation performance of polyvinylamine/polyacrylonitrile composite membrane. *J Chem Ind Eng. [in Chinese]*. 2003;54:1188–1191.
29. Dong CH, Wang Z, Yi CH, Wang SC. Preparation of polyvinylamine/polysulfone composite hollow-fiber membrane and their $CO_2/CH_4$ separation performance. *J Appl Polym Sci*. 2006;101:1885–1891.
30. Kim TJ, Li BA, Hägg MB. Novel fixed-site-carrier polyvinylamine membrane for carbon dioxide capture. *J Polym Sci*. 2004;42:4326–4336.
31. Deng LY, Kim TJ, Hägg MB. Facilitated transport of $CO_2$ in novel PVAm/PVA blend membrane. *J Membr Sci*. 2009;340:154–163.
32. Sandru M, Haukebø SH, Hägg MB. Composite hollow fiber membranes for $CO_2$ capture. *J Membr Sci*. 2010;346:172–186.
33. Zou J, Winston Ho WS. $CO_2$-selective polymeric membrane containing amines in crosslinked poly(vinyl alcohol). *J Membr Sci*. 2006;286:310–321.
34. Cai Y, Wang Z, Yi CH, Bai YH, Wang JX, Wang SC. Gas transport property of polyallylamine-poly(vinyl alcohol)/polysulfone composite membranes. *J Membr Sci*. 2008;310:184–196.
35. Matsuyama H, Terada A, Nakagawara T. Facilitated transport of $CO_2$ through polyethylenimine/poly (vinyl alcohol) blend membrane. *J Membr Sci*. 1999;163:221–227.
36. Deanna MD, Berend S, Jeffrey RL. Carbon dioxide capture: prospects for new materials. *Angew Chem Int Ed*. 2010;49:6058–6082.
37. Yu XW, Wang Z, Wei ZH, Yuan SJ, Zhao J, Wang JX, Wang SC. Novel tertiary amino containing thin film composite membranes prepared by interfacial polymerization for $CO_2$ capture. *J Membr Sci*. 2010;362:265–278.
38. http://riodb01.ibase.aist.go.jp/sdbs/cgi-bin/direct_frame_top.cgi.
39. Gunasekaran S, Anita B. Spectral investigation and normal coordinate analysis of piperazine. *Indian J Pure Appl Phys*. 2008;46:833–838.
40. http://www.chemicalbook.com/CAS_110-85-0.htm.
41. Carey FA. *Organic Chemistry*, 4th ed. New York: McGraw-Hill Higher Education, 2000: 863–864.
42. Bellamy LJ. *The infrared spectra of complex molecules*, 2nd ed. London and New York: Chapman Hall, 1980:20;179–187.
43. Noble RD, Koval CA. *Review of facilitated transport membranes*. In: Yampelskij Y, Pinnau I, Freeman B, editors. *Materials Science of Membranes for Gas and Vapor Separation*. Chichester, England: Wiley, 2006:411–436.
44. Wang Z, Li M, Cai Y, Wang JX, Wang SC. Novel $CO_2$ selectively permeating membranes containing PETEDA dendrimer. *J Membr Sci*. 2007;290:250–258.

45. Ruckenstein E, Shulgin I. Salting-out or -in by fluctuation theory. *Ind Eng Chem Res*. 2002;41:4674–4680.
46. Letcher TM. *Developments and Applications in Solubility*. UK: Royal Society of Chemistry, 2007.
47. Härtel G, Püschel Th. Permselectivity of a PA6 membrane for the separation of a compressed $CO_2/H_2$ gas mixture at elevated pressures. *J Membr Sci*. 1999;162:1–8.
48. Francisco GJ, Chakma A, Feng XS. Membranes comprising of alkanolamines incorporated into poly(vinyl alcohol) matrix for $CO_2/N_2$ separation. *J Membr Sci*. 2007;303:54–63.
49. Zhou C, Chung TS, Wang R, Liu Y, Goh SH. The accelerated $CO_2$ plasticization of ultra-thin polyimide films and the effect of surface chemical crosslinking on plasticization and physical aging. *J Membr Sci*. 2003;225:125–134.
50. Bos A, Pünt IGM, Wessling M, Strathmann H. Plasticization-resistant glassy polyimide membranes for high pressure $CO_2/CH_4$ separations. *Sep Purif Technol* 1998;14:27–39.
51. Bos A, Puènt IGM, Wessling M, Strathmann H. $CO_2$-induced plasticization phenomena in glassy polymers. *J Membr Sci*. 1999;155:67–78.
52. Visser T, Masetto N, Wessling M. Materials dependence of mixed gas plasticization behavior in asymmetric membranes. *J Membr Sci*. 2007;306:16–28.
53. Nunes SP, Peinemann KV. *Membrane Technology in the Chemical Industry*, 2nd ed. D-69469 Weinheim, Germany: Wiley-VCH Verlag GmbH, 2001.
54. Wei XY, Wang Z, Chen J, Wang JX, Wang SC. A novel method of surface modification on thin-film-composite reverse osmosis membrane by grafting hydantoin derivative. *J Membr Sci*. 2010;346:152–162.
55. Shintani T, Matsuyama H, Kurata N. Development of a chlorine-resistant polyamide reverse osmosis membrane. *Desalination*. 2007;207:340–348.
56. Yang DX, Wang Z, Wang JX, Wang SC. Parametric study of the membrane process for carbon dioxide removal from natural gas. *Ind Eng Chem Res*. 2009:48;9013–9022.

*Manuscript received Sept. 30, 2011, and revision received Feb. 7, 2012.*